Influence of the trailing edge shape on the aerodynamic characteristics of an airfoil at low Re number using RANS

R. Perrin, P. Rattanasiri, Eric Lamballais, S. Yooyen

IOP Conference Series: Materials Science and Engineering

Influence of the trailing edge shape on the aerodynamic characteristics of an airfoil at low Re number using RANS

Influence of the trailing edge shape on the aerodynamic characteristics of an airfoil at low Re number using RANS

R. Perrin[1,2,*], P. Rattanasiri[3], E. Lamballais[4] and S. Yooyen[2]

[1]Department of Mechanical Engineering, Faculty of Engineering at Sriracha, Kasetsart University Sriracha Campus, Sriracha, Chonburi 20230, Thailand
[2]Department of Aeronautical Engineering, International Academy of Aviation Industry, King Mongkut's Institute of Technology Ladkrabang, Bangkok 10520, Thailand
[3]Department of Mechanical Engineering, Faculty of Engineering, Burapha University, Chonburi, 20131, Thailand
[4]Institute PPRIME, Department of Fluid Flow, Heat Transfer and Combustion, CNRS Université de Poitiers ENSMA, Téléport 2, Futuroscope Chasseneuil Cedex, France

* Corresponding Author: rodolphe.perrin@univ-poitiers.fr

Abstract
Recent studies have demonstrated that periodic spanwise modifications of the Trailing Edge of an airfoil can significantly reduce the noise produced and can also increase its aerodynamic performances. This study aims to analyse the effects of such modifications on the aerodynamic performances of a profile by numerical simulation, with a particular emphasis on low Reynolds numbers typical of Unmanned Aerial Vehicles, Micro Aerial Vehicle, and/or small wind turbines. In the range of Re numbers considered here, the flow presents laminar separation eventually followed by transition and reattachment (depending on Reynolds number, Angle of Attack and Free Stream Turbulence).
As the standard for industrial applications is still the RANS approach, thanks to its moderate computational cost, this approach is considered here and a first step consists in evaluating the ability of recently proposed transition models (Menter, 2015; Ge, 2014; Kubacki, 2016) to predict the characteristics of the flow for such geometries. A baseline NACA0012 profile is considered, together with modified Trailing Edges (blunt and serrated). Simulations are performed using Code_Saturne (2nd order finite volume), and the influence of the Free Stream Turbulence, Angle of Attack, and Reynolds number on the aerodynamics performances is examined. The results are compared with data from the literature.

1. Introduction

This paper is a first step of a study on the effect of Trailing Edge (henceforth TE) modifications on the aerodynamic performances of wings at low Reynolds number. The specific objective is to assess the performances of recently proposed RANS transition models ([1-3]) by making a comparison with results from the literature. NACA0012 profiles, with baseline and modified TE, are considered and the influence of Angle of Attack (henceforth AoA), Re number and Free Stream Turbulence (henceforth

FST) are examined. The configuration and numerical set-up are described in the following section. Section 3 presents the main results and conclusions and perspectives are given in Section 4.

2. Configuration and numerical set-up

The three airfoils analysed in the study of [4] using Direct Numerical Simulation (henceforth DNS), are considered: a standard NACA0012 with straight TE (denoted 'baseline TE' in the following), a blunt TE airfoil which is obtained by truncating the NACA0012 profile at a distance $0.133c$ from the TE of the baseline airfoil (where c is the chord of the baseline airfoil) and a serrated cut-in TE with a triangular shape and spanwise wavelength of $0.266c$, as shown in Figure 1. At a trough of the serrated TE airfoil, the cross-section is the same as the blunt TE one, and at a peak, the cross-section is the same as the standard NACA0012 one.

Simulations are carried out using the open-source CFD software called *Code_Saturne,* developed by EdF (see http://www.code-saturne.org). The software is based on a 2nd order accurate finite volume method using a collocated arrangement on unstructured grids and velocity-pressure coupling is performed using a predictor-corrector algorithm of SIMPLEC type. In the present study, a 2nd order upwind scheme is selected for the convection terms of each transport equation.

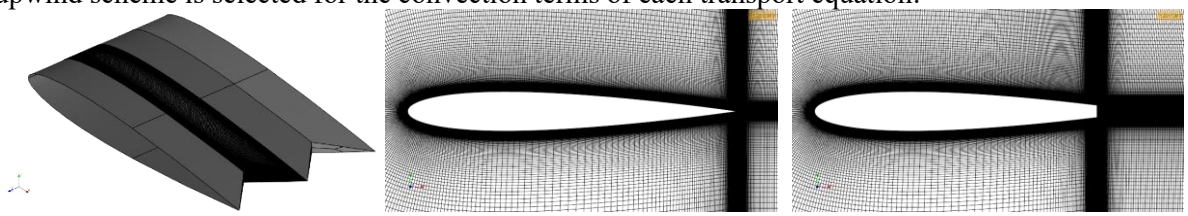

Figure 1. Geometry of the serrated TE (left) and mesh at a peak (middle) and at a trough (right).

Meshes have been generated using the open-source platform *Salome*. A C-type grid topology is employed. The computational domain extends a radius $20c$ around the leading edge and the outlet boundary is located $20c$ downstream the trailing edge. 2D simulations are carried out for the baseline TE and blunt TE cases, and grids of 140000 to 160000 cells have been found necessary for these cases. Grids are refined in the direction normal to the walls so that $y^+ \leq 1$ at the walls and the number of points around the surface of the airfoil is 438, with a higher density on the upper surface to resolve the separation, transition and reattachment. For the 3D simulations (serrated TE), the domain extends half a wavelength in the spanwise direction (symmetry conditions are used on the span boundaries) and the mesh contains 11 million cells.

RANS transition models from [1], [2] and [3] have been implemented in *Code_Saturne* and compared in this paper. Each model is based on a $k-\omega$ model (SST in the case of [1]). Models [1] and [3] uses a transport equation for the intermittency γ, designed so that $\gamma = 0$ in the laminar regions of the boundary layer and increases to 1 in the turbulent regions after the transition. The variable γ mainly acts on the original turbulence model by weighting the production term in the equation for k. In the model by [2], γ is given by an algebraic relation and other modifications are made in the original model. A detailed description of the equations of each model can be found in the original papers.

The angle of attack is introduced through the free-stream velocity vector imposed on the external boundary. Concerning the turbulent variables k and ω, inlet values at a distance of $20c$ upstream of the leading edge are first selected, and the analytical solution of the $k-\omega$ model corresponding to the case of decaying isotropic turbulence is imposed on the external boundary. The inlet values are chosen to impose a FST intensity $Tu=u'/U$ at the leading edge location.

As explained in the following sections, simulations with different Re, Tu and TE shape are carried out. For each case, AoA is varied from 0° to 12° by steps of 1°. Although not discussed in the paper, some of the cases considered are unsteady mainly because of the presence of a vortex shedding in the wake. For these cases the simulations are carried out until a statistically steady regime is reached and

averages are computed. In the following, all quantities are made dimensionless using the inflow velocity and the chord of the baseline airfoil.

3. Results

3.1 Comparison with reference data for the baseline case at Re=50000

The models by Menter et al [1], Kubacki et al [2] and Ge et al [3] are first compared with reference data for the baseline TE NACA0012 at Re=50000. As noted by [5], a lot of disagreements is found between published experimental results in the literature, mainly because at this low Reynolds number, the flow is very sensitive to small variations of external conditions. Recently, Direct Numerical Simulations and Large Eddy Simulations could be performed for this case and the DNS results of [6] (at AoA=5° and 8°) will be used here as a reference for comparison between the models. The experimental results of [5] are also selected for comparison because of their reasonable agreement with the DNS results.

Figure 2 presents the iso-contours of the U-component of the velocity and streamlines obtained with the model by Kubacki et al., [2] at AoA=5°. As can be seen, the presence of a separation bubble on the suction side can be identified. Although not shown in the paper, visualisation of the turbulent kinetic energy and intermittency, for instance, clearly shows a laminar separation, followed by transition and turbulent reattachment, in agreement with the literature.

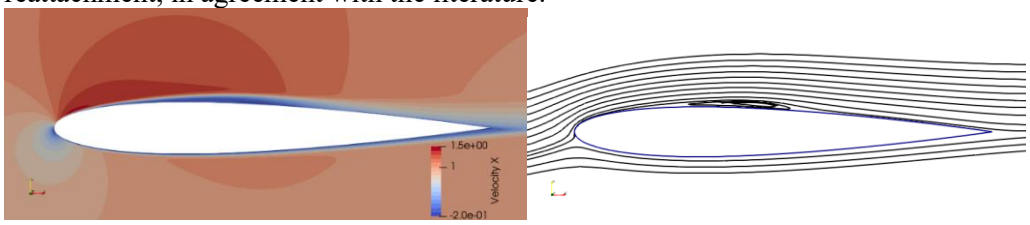

Figure 2. Iso-contours of U (left) and streamlines (right) at Re=50000; AoA=5° predicted by the model of Kubacki et al (2016).

Figure 3 (on the left side) shows the mean lift and drag coefficients for different AoA, which are predicted by the different models. One aspect consistently reported in the literature is the nonlinearity of the curve *Cl*(*AoA*) at low Re, which contrasts with results from the thin airfoil theory. It appears that this aspect is better predicted by the models by [1] and [2]. In particular, the model by [1] predicts the negative slope of *Cl*(*AoA*) at very low AoA reported by the experiment (smaller steps in AoA should be considered to assess if this behaviour is also predicted by the model by [2]). Except at very low AoA, the model by [2] achieves the best agreement with experimental values on a large range of AoA. The nonlinear character of the lift curve is poorly predicted by the model given in [3]. Furthermore, a very long time of convergence was needed in comparison with the computations using the other models. Thus, only the models provided in [1] and [2] have been considered in the following.

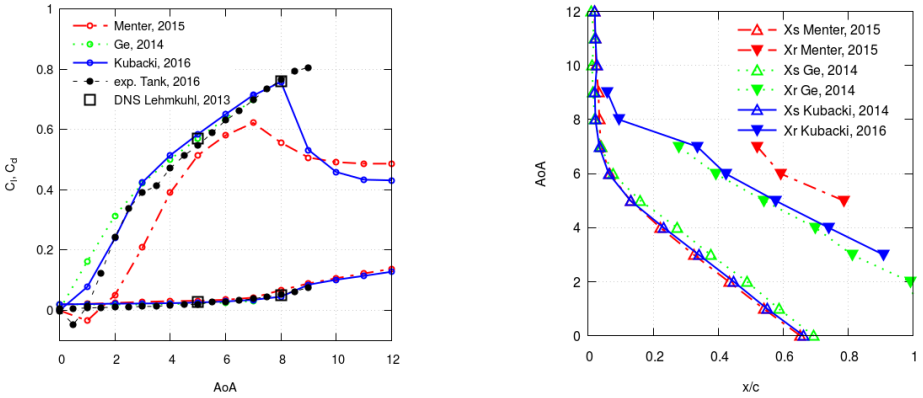

Figure 3. Comparison of models; left: lift and drag coefficients *Cl* and *Cd*; right: locations of separation *Xs* and reattachment *Xr*

Figure 3 (on the right side), shows the position of the separation and reattachment (identified using the mean friction coefficient) for different AoA. In agreement with the literature, e.g. [7], it is first observed that no reattachment occurs at low AoA, and that for AoA>3°, both separation and reattachment moves towards the leading edge when AoA increases. It is also seen that the decrease of the length of the separation bubble with AoA, reported in the literature, is well predicted. Regarding the comparison of the models, it is clearly observed that the reattachment predicted using the model in [1] is strongly delayed comparing to the one predicted by the model [2].

A closer analysis can be done from Figure 4 and Figure 5, which represent the pressure and friction coefficients *Cp* and *Cf* from both models and compared to DNS results from [6] at AoA=5° and AoA=8°.The shape of the profiles of *Cp* and *Cf* are typical of laminar separation bubbles with transition followed by reattachment. The start of the constant pressure region ("plateau") is located close to the separation, the end of the plateau is close to the transition, and the point at which the rate of the pressure recovery changes is found close to the reattachment. Concerning the *Cf* profile, low negative values are found in the laminar region of the bubble upstream of transition and an increase of |*Cf*| values is observed after the transition, before the mean reattachment. At AoA=5°, an excellent agreement is achieved with the DNS results using the model from [2]. The model by [1] appears to predict correctly the location of separation and transition, but the rate of the pressure recovery appears too slow after the transition and the position of the reattachment is predicted too much downstream. Thus, it appears that while the start of the transition is well predicted by the model by [1], this transition is too slow and delays the reattachment. This also explains why no reattachment is observed (on figure 2 right) using this model for AoA<5°, contrary to the results of the other models. At AoA=8°, the same default is observed with the model by [1] concerning the region after transition and the best agreement with DNS is also achieved by the model [2] concerning the *Cp* profile. However, it can be noticed on the *Cf* profiles that the transition appears too early with the model by [2], while the location of the start of transition is well predicted by the model by [1].

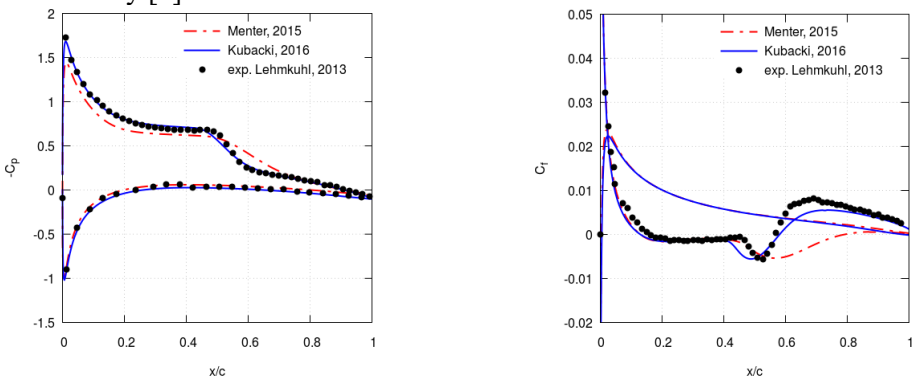

Figure 4. Pressure coefficient *Cp* (left) and friction coefficient *Cf* (right) at Re=50000; AoA=5°

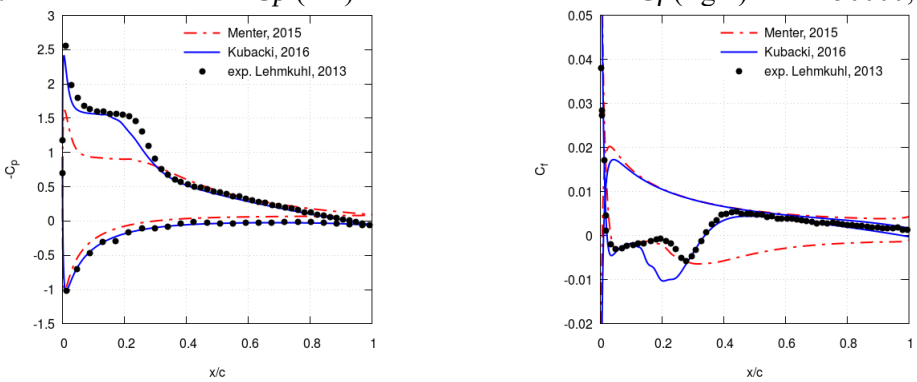

Figure 5. Pressure coefficient *Cp* (left) and friction coefficient *Cf* (right) at Re=50000; AoA=8°

3.2 Reynolds number influence

In this section, the effect of a variation of the Reynolds number in this regime is examined by comparing the precedent results (at Re=50000) with simulations at Re=100000, and for the same Free Stream Turbulence characteristics. According to the literature (e. g. [7]), an increase in Re number from 50000 to 100000 results in a slight shift of the separation in the downstream direction (for AoA at which the bubble is present) and a significant shift of the reattachment toward the upstream direction, which can be explained by an earlier transition. This results in a shorter separation bubble length. Concerning the aerodynamic performances, this increase of Re number results in a higher maximum lift coefficient, which happens at a higher stall AoA.

Figure 6 (on the left side) shows the lift and drag coefficients whilst Figure 6 (on the right side) reports the positions of separation and reattachment predicted by both models at different AoA. It can be seen that the trends reported in the literature are well predicted by both models, except the slight shift of the separation predicted by the model from [1]. It is also noticeable that the two models are in much better agreement at Re=100000 than at lower Re. Particularly, it is observed that the reattachment occurs at much lower AoA, and that the nonlinearity of the *Cl* curve is strongly reduced with the increase of Re number.

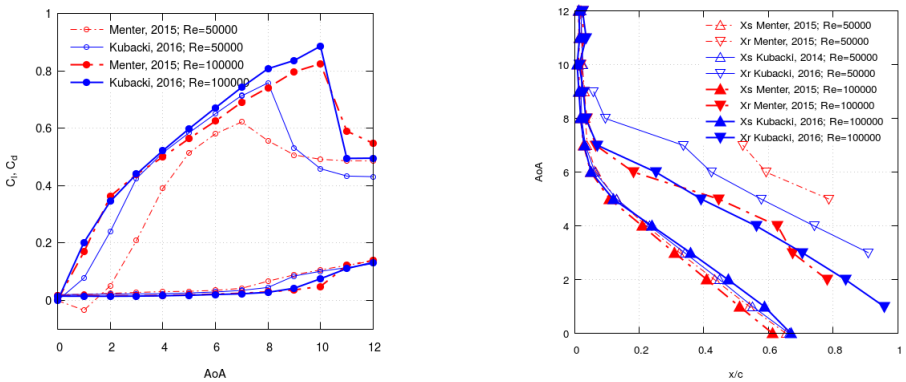

Figure 6. Influence of Reynolds number: *Cl* and *Cd* (left) and positions *Xs* and *Xr* (right).

3.3 Free Stream Turbulence intensity influence

According to [7] and other references, it is generally accepted that increasing the Free Stream Turbulence intensity results in effects similar to that obtained by increasing the Re number. While an increase in FST intensity delays separation, the transition and reattachment occur earlier, and the resulting separation bubble is significantly shorter. An increase of the maximum lift coefficient and stall angle of attack is also reported in the literature. Figure 7 presents aerodynamic coefficients, as well as separation and reattachment positions predicted by both models for different turbulent intensities $Tu=u'/U$ (measured at the leading edge). For both models, no difference is obtained by lowering the turbulence intensity compared to that imposed in the previous sections. For increased *Tu*, no increase in the maximum lift coefficient and stall angle is observed for both models. The model by [1] predicts a slightly delayed separation, as well as an earlier reattachment, in agreement with the literature. In contrast, very minor changes are observed using the model by [2].

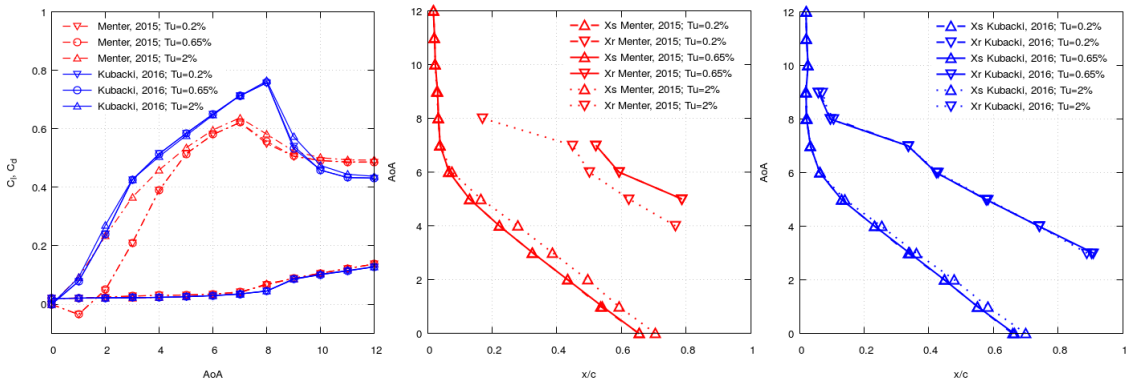

Figure 7. Influence of Free Stream Turbulence: *Cl* and *Cd* (left) and positions *Xs* and *Xr* using the model of Menter et al (2015) (middle) and the model of Kubacki et al (2016) (right)

3.4 Trailing Edge shape influence

In this section, the prediction of the flow around wings with a modified TE is analysed. The same geometries as in [4], which uses DNS, are selected for comparison and assessment of the models. The results for the blunt TE are presented in Figure 8 and Figure 9 (on the left side). It is reminded that the lift and the drag from all cases are made dimensionless using the chord of the baseline airfoil. It can be seen from the figures that the position of separation and reattachment are only slightly modified by the TE modification both being slightly shifted toward the downstream area, in agreement with [4]. Concerning the lift coefficient, both models are in better agreement at low AoA, for which no reattachment occurs. It is also noticeable that a small increase of the stall angle is predicted by the model in [2], in line with results reported in the literature.

Concerning the pressure coefficient profile at AoA=5°, the most noticeable feature is a reduction of the minimum *Cp* for the blunt TE, compared to the baseline TE (see Figure 9 on the left side). This effect, well predicted by both models, is in good agreement with the results of [4]. As [4] explains that the origin of this behaviour is inviscid, it is not surprising that simulations with both models predict well this effect. Although not shown in the paper because of space limitation, it is also noticeable that a vortex shedding is predicted by the model by [2] in the wake, which has to be associated with the bluntness of the TE, also in good agreement with the results of [4]. This shedding is not predicted by the model of [1] (the predicted flow is steady), probably because of the different wake velocity profile resulting from the too long transition and delayed reattachment discussed in section 3.1.

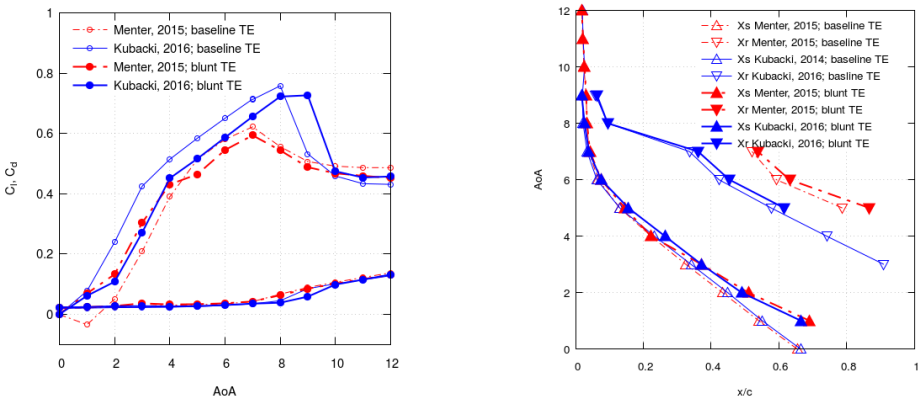

Figure 8. Influence of Trailing shape: lift and drag coefficient (left) and position of separation and reattachment (right) for the baseline and blunt trailing edge.

The pressure coefficient obtained for the serrated TE (3D) case is represented at the spanwise locations of a peak and a trough in Figure 9 (on the right side). It is reminded that the section of the wing at a trough corresponds to the blunt TE geometry. In agreement with the results of [4], the pressure distribution is almost identical at peak and trough spanwise locations in the upstream part of the wing.

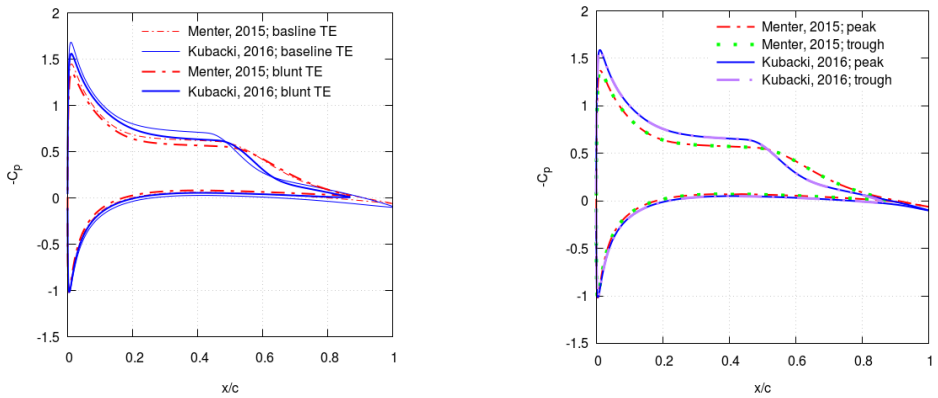

Figure 9. Influence of Trailing Edge shape: pressure coefficient *Cp* (Re=50000; AoA=5°); left: baseline and blunt trailing edge; right: serrated trailing edge (*Cp* at peak and trough).

4. Conclusion and perspectives

As a first step of a study on the effects of TE modification of airfoil at low Re number using RANS, the models by Menter et al [1], Kubacki et al [2] and Ge et al [3] were implemented in Code_Saturne and assessed for the flow around a NACA0012 profile, for different Re, different Tu and different TE. For the cases considered here at Re=50000, the model by [2] leads to the closest agreement with results from the literature (e.g. [6]), while the model by [1] predicts a too slow transition. However, the effects of the variations of parameters such AoA and Tu seems to be better predicted by the model of [1], especially considering the start of the transition. Although further investigation would be necessary, it is possible that a recalibration of some terms in the model of [1] for low Re case would allow better predictions. Concerning the TE modification effect, a close agreement has been achieved with the results of [4] and it is therefore expected that the used model will be suitable for a more detailed study on the effects of spanwise wavelength and amplitude of the serrations.

Acknowledgments

Computations have been performed on the supercomputer facilities of the “Mésocentre de calcul de Poitou Charentes”.

References

[1] Menter F R Smirnov P E Liu T and Avancha R 2015 *Flow, Turbulence and Combustion* **95**(4) 583-619
[2] Kubacki S and Dick E 2016 *International Journal of Heat and Fluid Flow* **62** 344-361
[3] Ge X Arolla S and Durbin P 2014 *Flow, turbulence and combustion* **93**(1) 37-61
[4] Thomareis N and Papadakis G 2017 *Physics of Fluids* **29**(1) 014101
[5] Tank J Smith L and Spedding G R 2017 *Interface focus* **7**(1) 20160076
[6] Lehmkuhl O Rodríguez I Baez A Oliva A and Pérez-Segarra C D 2013 *Computers & Fluids* **84** 176-189
[7] Huang R F and Lee H W 1999 *Journal of aircraft* **36**(6) 965-972